Magnetite L-proline as a reusable nano-biocatalyst for efficient synthesis of 4H-benzo[b]pyrans in water: a green protocol

Hamideh Aghahosseini[a,b],*, Ali Ramazani[a,b]

[a]Department of Chemistry, University of Zanjan, P O Box 45195-313, Zanjan, Iran

[b]Research Institute of Modern Biological Techniques (RIMBT), University of Zanjan, P O Box 45195-313, Zanjan, Iran

Abstract

L-Proline is known as the most favored organocatalyst in enamine-mediated reactions. Magnetic functionalization of this organocatalyst could solve its recovery and reuse problems. Herein we report the use of magnetic L-proline nano-biocatalyst for a simple and efficient one-pot coupling reaction of dimedone, malononitrile, and aromatic aldehydes to afford the corresponding tetrahydrobenzo[*b*]pyrans as a significant class of heterocyclic compounds with great biological and pharmacological importance according to a green protocol. Low cost, facile handling, simple preparation, high stability, reusability, and low toxicity are some remarkable features of this nano-biocatalyst.

Keywords: L-proline; magnetic functionalization; nano-biocatalyst; reusability; tetrahydrobenzo[*b*]pyrans.

Introduction

L-proline has been known as a highly efficient and versatile organocatalyst [1-3] that could contrast with the complex natural enzymes in the context of promoting similar transformations. From this point of view, proline is termed "the simplest enzyme" [4]. The enhanced nucleophilicity of L-proline over the other amino acids raised from the secondary amine functionality in its pyrrolidine ring.

Iron oxide magnetic nanoparticles have become one of the most important field of nanomaterial science. Magnetic nanoparticles can be stabilized and chemically functionalized. The simple recoverability and reusability of magnetic nanoparticles caused their highly broad applications as catalyst supports. In addition, they have the advantages of high surface area, good dispersion, and stability [5-7].

Tetrahydrobenzo[b]pyrans as a major class of natural heterocyclic compounds have shown wide biological properties such as antibacterial, antimicrobial, anti-cancer, anti-HIV, and anti-anaphylactic [8-12]. They have attracted a considerable attention from researchers for the development of significant preparation methods for these important heterocyclic compounds. Among the several synthetic methods which were

*Corresponding author: H. Aghahosseini

Tel: +98 (24) 33052635, Fax: +98 (24) 33052635
E-mail: hamideh.aghahosseini@gmail.com

introduced for the production of tetrahydrobenzo[*b*]pyrans [8,13-35]. However, some of them have drawbacks, such as the use of volatile organic solvents, the existence of toxic metals in their catalyst structure, the use of complicated or expensive catalyst preparation procedures, low yields, and long reaction time.

Herein we report the multi component condensation between aldehydes, malononitrile and dimedone using magnetic L-proline (Fe_3O_4@L-proline) as an efficient, reusable and low cost nano-biocatalyst under the green conditions.

Experimental

General

All the chemicals were purchased from commercial suppliers and used without more purification. NMR spectra were measured on a Bruker 250 MHz spectrometer. IR-Spectra were recorded on a Perkin-Elmer FT-IR Spectrum, using KBr pallets. The magnetic properties of Fe_3O_4@L-proline were detected at room temperature using VSM (VSM, Meghnatis Kavir Kashan Co., Kashan, Iran). The structural properties of Fe_3O_4@L-proline were determined by XRD with a X'Pert-PRO advanced diffractometer using Cu (Ka) radiation (wavelength: 1.5406 Å), operated at 40 kV and 40 MA from 10 to 80° at room temperature. The particle size and morphology of the Fe_3O_4@L-proline was investigated by FE-SEM (TE-SCAN, Brno Czech Republic). The EDAX spectrum of Fe_3O_4@L-proline was recorded by the EDAX detector which was mounted on the FE-SEM. Thermal properties of Fe_3O_4@L-proline analyzed by TGA (Perkin Elmer, model: pyris Diamond) at the heating rate of 20°C min^{-1} over the temperature range of room temperature to 800 °C.

Preparation of Fe_3O_4@L-proline

Fe_3O_4@L-proline was produced according to the method reported by Safaei-Ghomi [36]. In a 250 mL beaker containing distilled water (120 mL), $FeCl_3$ (0.97 g), $FeSO_4.7H_2O$ (0.9 g) and L-proline (0.9 g), a solution of 1.5 M NH_4OH (120 mL) were added dropwise with vigorous stirring at 100 °C under N_2 atmosphere until the pH was raised to 11 and a black precipitate was formed. Then the reaction was refluxed for 6 h under vigorous stirring and obtained Fe_3O_4@L-proline magnetic nanocatalyst was easily separated from the reaction mixture by simple magnetic decantation. Then the mixture was washed several times with distilled water and ethanol, and then dried in a vacuum oven at 60 °C for 2 h. The L-proline content in the Fe_3O_4@L-proline nanocatalyst was 4.68 mmol.g^{-1} [36].

General procedure for the synthesis of 4H-benzo[b]pyrans

The mixture of aldehyde (1 mmol), malononitrile (1.2 mmol), and Fe_3O_4@L-proline nanocatalyst (0.02 g, 1.2 mol%) was added to water (5 mL), and heated under refluxing conditions for a few minutes, and then dimedone (1 mmol) was added and the mixture was stirred for 10-15 min. The progress of the reaction was monitored using thin-layer chromatography TLC. After the reaction completed, the catalyst was recovered using an external magnet and the solid product was collected by filtration, and then recrystallized from hot ethanol to afford pure products.

Spectral data for selected compounds:
2-Amino -7, 7-dimethyl-4-(2-nitrophenyl)-5-oxo-5, 6, 7, 8-tetrahydro-benzo[b]pyran (4e)
IR (KBr): vmax=3471 (NH_2), 3334 (NH_2), 2192 (C≡N), 1663 (C=O), 1213 (C–O). ^{1}H NMR (250.13 MHz, DMSO-d_6) δ_H 7.79 (d, *J*=7.75 Hz, 1H), 7.61 (t, *J* =7.00 Hz, 1H), 7.40 (t, *J*=7.00 Hz, 1H),

7.33 (d, *J*=7.75 Hz, 1H), 7.18 (s, 2H), 4.91 (s, 1H), 2.18 (d, *J*= 16.01 Hz, 2H), 1.99 (d, *J*= 16.01 Hz, 2H), 0.99 (s, 3H), 0.85 (s, 3H); ^{13}C NMR (62.90 MHz, DMSO-*d₆*) δ_C 27.1, 28.7, 30.3, 32.2, 50.0, 56.7, 112.7, 119.5, 124.1, 128.3, 130.7, 133.8, 139.3, 149.4, 159.6, 163.1, 196.2.

2-Amino -7, 7-dimethyl-4-(4-nitrophenyl)-5-oxo-5, 6, 7, 8-tetrahydro-benzo[b]pyran (4f)

IR (KBr): vmax=3408 (NH$_2$), 3318 (NH$_2$), 2183 (C≡N), 1670 (C=O), 1215 (C–O). ^{1}H NMR (250.13 MHz, DMSO-*d₆*) δ_H 8.14 (d, *J*=8.00 Hz, 2H), 7.42 (d, *J* =8.00 Hz, 2H), 7.17 (s, 2H), 4.34 (s, 1H), 2.24 (d, *J*=16.01 Hz, 2H), 2.08 (d, *J*=15.01 Hz, 2H), 1.01 (s, 3H), 0.93 (s, 3H); ^{13}C NMR (62.90 MHz, DMSO-*d₆*) δ_C 27.3, 28.6, 32.2, 36.0, 50.2, 57.4, 112.1, 119.7, 124.1, 129.0, 146.7, 152.7, 159.0, 163.5, 196.1.

2-Amino -7, 7-dimethyl-4-(1H-pyrrol-2-yl)-5-oxo-5, 6, 7, 8-tetrahydro-benzo[b]pyran (4i)

IR (KBr): vmax=3416 (NH$_2$), 3198 (NH$_2$), 2925 (C-H), 2193 (C≡N), 1675 (C=O), 1198 (C–O). ^{1}H NMR (250.13 MHz, DMSO-*d₆*) δ_H 8.39 (s, 2H), 7.51 (m, Ar-H), 7.31 (m, Ar-H), 7.11 (m, Ar-H), 4.24 (s, 1H), 2.24 (d, *J*=15.76 Hz, 2H), 2.12 (m, 2H), 1.01 (s, 3H), 0.92 (s, 3H); ^{13}C NMR (62.90 MHz, DMSO-*d₆*) δ_C 27.3, 28.6, 32.2, 33.8, 50.3, 57.7, 112.2, 119.9, 124.1, 135.2, 140.4, 148.2, 149.1, 159.0, 163.4, 196.2.

Results and discussion

Characterization of Fe₃O₄@L-proline nanocatalyst

The Fe$_3$O$_4$@L-proline nanocatalyst was prepared and characterized using FT-IR, SEM, EDAX, TGA as well as XRD which was in good agreement with those in the literature [36].

The FT-IR spectra of the Fe$_3$O$_4$ nanoparticles, L-proline and Fe$_3$O$_4$@L-proline nanocatalyst are represented in Figure 1. The Fe$_3$O$_4$@L-proline nanocatalyst represented an intense peak at 1628 cm^{-1} which is derived from C=O stretching of L-proline and the peak at 583 cm^{-1} is raised from Fe–O bond of Fe$_3$O$_4$ nanoparticles. The wavenumber separation between the asymmetric and symmetric COO$^-$ group in FT-IR bands can be used to distinguish the type of interaction between the carboxylate head and the metal atom [37]. According to Zhang *et al.* findings, this wavenumber separation value in our work [$\upsilon_{asymmetric}$ (1628) - $\upsilon_{symmetric}$ (1363)= 265 cm^{-1}] indicates the monodentate interaction between the carboxylate head and the Fe in chemisorbtion of L-proline onto the Fe$_3$O$_4$ nanoparticles [37].
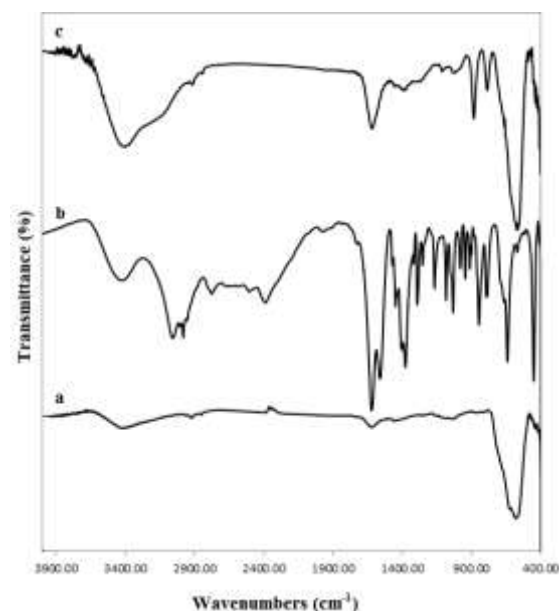

Figure 1. FT-IR spectra of Fe$_3$O$_4$ (a), L-proline (b) and Fe$_3$O$_4$@L-proline nanoparticles (c).

The SEM image showed that average size of the synthesized Fe$_3$O$_4$@L-proline particles was about 20-30 nm, and they had a spherical morphology (Figure 2).
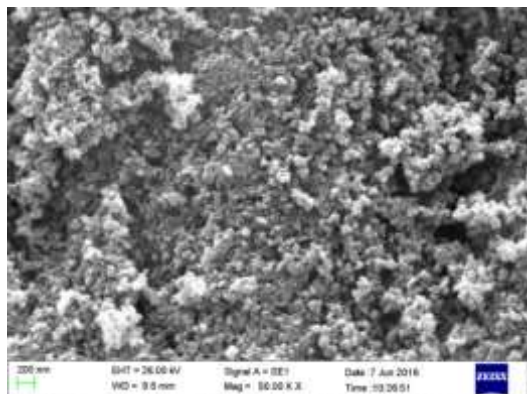
Figure 2. SEM image of Fe$_3$O$_4$@L-proline nanoparticles.

The EDAX spectrum for the Fe$_3$O$_4$@L-proline nanocatalyst is illustrated in Figure 3. Only carbon (C), nitrogen (N), oxygen (O) and iron (Fe) signals can be observed.
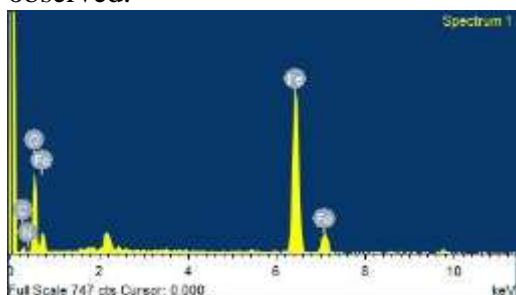

Figure 3. The EDAX spectrum (a) and elemental composition (b) of Fe$_3$O$_4$@L-proline nanocatalyst**.**

Thermal decomposition analysis of Fe$_3$O$_4$ and Fe$_3$O$_4$@L-proline nanoparticles was investigated by TGA analysis (Figure 4). The first weight loss from 25 °C to 170 °C was due to the removal of surface-adsorbed water. The other weight loss steps confirmed the cleavage of L-proline moiety. The magnetic functionalization of L-proline increased its thermal stability. The complete decomposition temperature of the pristine L-proline was reported below 264 °C [38], whereas Fe$_3$O$_4$@L-proline

represented higher thermal stability (Figure 4). Therefore, it was found that, the L-proline moieties covalently linked onto the surface of Fe$_3$O$_4$ nanoparticles. The L-proline content in the Fe$_3$O$_4$@L-proline was 0.61 mmol.g^{-1}, which was determined according to the weight loss steps from TGA analysis.
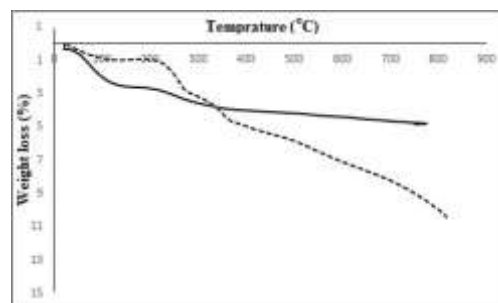

Figure 4. The TGA thermograms of Fe$_3$O$_4$ (solid line) and Fe$_3$O$_4$@L-proline nanocatalyst (dash line)

X-ray diffraction patterns of the nanoparticles are demonstrated in Figure 5. The XRD pattern of the Fe$_3$O$_4$@L-proline represents diffraction peaks at 2θ of 29.96°, 35.41°, 42.98°, 53.32°, 56.99° and 62.63° corresponding to the spinel structure of Fe$_3$O$_4$ (ref. code 00-002-1035), as shown in Figure 5. The broad peaks in XRD pattern could be related to the cubic structure of Fe$_3$O$_4$.

The full width at half maximum (FWHM), Miller indices, size and inter-planer distance of Fe$_3$O$_4$@L-proline were calculated in the 29.9° to 74.1° range (Table 1). According to the Scherrer equation [$D = K\lambda/(\beta\cos\Theta)$] and the Bragg equation [$d_{hkl} = \lambda/(2\sin\Theta)$] the crystallite size and the inter-planer distance for the highest diffraction line (35.4°) in Fe$_3$O$_4$@L-proline were obtained 12.3 and 0.253 nm, respectively.
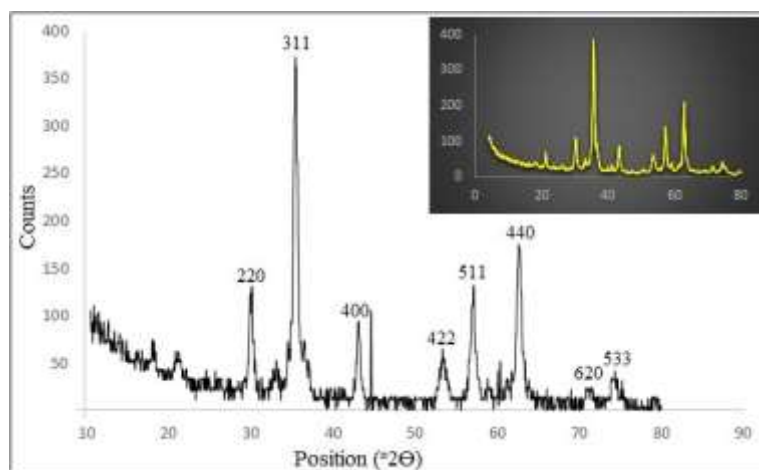
Figure 5. XRD patterns of Fe_3O_4 (top part of figure) and Fe_3O_4@L-proline nanocatalyst.

Table 1. XRD data for the Fe_3O_4@L-proline nanocatalyst.

Entry	2Θ	Peak width (FWHM)	Miller indices			Particle Size (nm)	Inter-planer distance (nm)
			h	k	l		
1	29.9	0.492	2	2	0	16.7	0.298
2	35.4	0.683	3	1	1	12.3	0.253
3	42.9	0.344	4	0	0	24.8	0.21
4	53.3	0.590	4	2	2	15.1	0.172
5	56.9	0.492	5	1	1	18.4	0.161
6	62.6	0.442	4	4	0	21	0.148
7	71.0	0.984	6	2	0	9.9	0.133
8	74.1	0.720	5	3	3	13.8	0.128

Catalytic activity

We investigated the catalytic performance of the Fe_3O_4@L-proline in the synthesis of 4*H*-benzo[*b*]pyrans (Figure 6).

The FWHM, Miller indices, size, and inter-planer distance of the Fe_3O_4@L-proline were calculated in the 29.9 to 74.1 range (Table 1). According to the Scherrer equation [$D=K\lambda/(\beta cos\Theta)$] and the Bragg equation [$d_{hkl}=\lambda/(2sin\Theta)$] the crystallite size and the inter-planer distance for the highest diffraction line (35.4°) in Fe_3O_4@L-proline were obtained 12.3 nm and 0.253 nm, respectively.
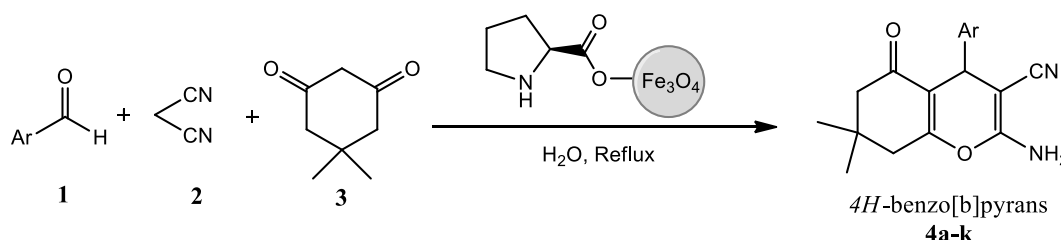

Figure 6. The synthesis of 4H-benzo[*b*]pyrans.

In a plausible mechanism (Figure 7), at first, magnetite L-proline in a reaction with an aromatic aldehyde could form iminium ion **5**. The obtained iminium ion could facilitate the condensation between aromatic aldehyde **1** and malononitrile **2**, that afford olefin **7** via the dehydration of intermediate **6.** On the other hand, the magnetite L-proline could produce enamine intermediate **8** via the reaction with dimedone. Then the enamine intermediate **8** is reacted with olefine **7**

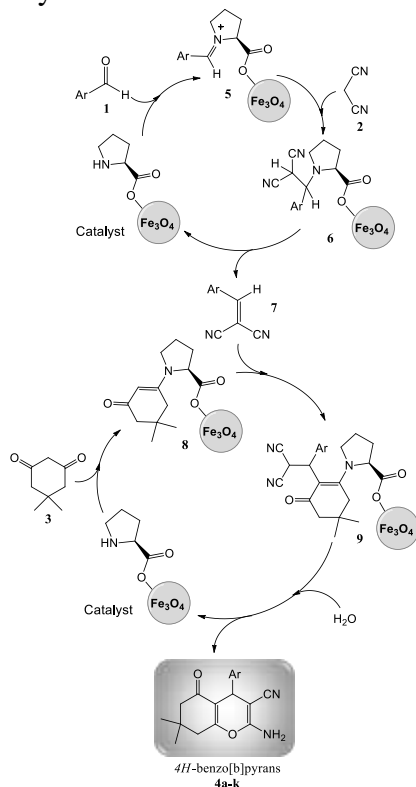and the product **4** is generated via the hydrolysis of intermediate **9**.

Figure 7. Possible mechanism for the Fe$_3$O$_4$@L-proline-catalysed synthesis of tetrahydrobenzo[*b*]pyran derivatives

The catalytic performance of Fe$_3$O$_4$@L-proline for the synthesis of tetrahydrobenzo[*b*]pyrans was evaluated according to a green protocol. The reaction conditions were optimized according to the condensation of 4-nitrobenzaldehyde, malononitrile and dimedone in water as a model reaction using different amounts of Fe$_3$O$_4$@L-proline in the room temperature and reflux conditions. As shown results in Table 2, the use of 0.02 gr Fe$_3$O$_4$@L-proline under reflux conditions leads to the best results from the reaction time and yield point of view.

Table 2. The effects of the amount of Fe$_3$O$_4$@L-proline nanocatalyst and temperature on the condensation of 4-nitrobenzaldehyde (1 mmol), malononitrile.

Entry	Catalyst amount (g)	Temp (°C)	Time (min)	Yield[a] (%)
1	0.01	110	10	85
2	0.02	110	10	100
3	0.03	110	10	98
4	0.02	25	120	10
5	0	110	600	10

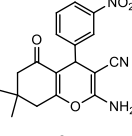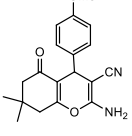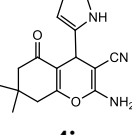(1.2 mmol), and dimedone (1 mmol) in water (4 mL)
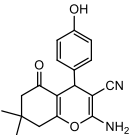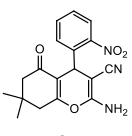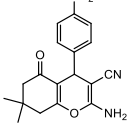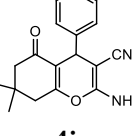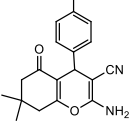
[a] Isolated yield

We extended our investigation using Fe$_3$O$_4$@L-proline with different precursors to prepare series of 4*H*-benzo[*b*]pyrans (Table 3).

inter-planer distance for the highest diffraction line (35.4°) in Fe$_3$O$_4$@L-proline were obtained 12.3 nm and 0.253 nm, respectively

Table 3. The Fe$_3$O$_4$@L-proline-based catalytic synthesis of 4*H*-benzo[*b*]pyrans[a].

Entry	Product	Yield[b](%)	Time (min)	m.p. (°C)	Ref
1	**4a**	93	15	226-228	[39]
2	**4b**	89	10	223-224	[26]
3	**4c**	86	10	215-218	[40]

4	4d	82.5	15	214-216	[22]
5	4e	76.3	15	234-236	[40]
6	4f	70	10	175-176	[20]
7	4g	64.5	15	201-205	[41]
8	4h	60.8	15	199-201	[41]
9	4i	65	15	178-180	-
10	4j	44	15	233-235	[41]
11	4k	49	15	209-211	[26]

[a]Reaction conditions: aromatic aldehydes (1 mmol), dimedone (1 mmol), malononitrile (1.2 mmol), Fe_3O_4@L-proline nanoparticle (0.02 g), water (5 mL), reflux;
[b]Isolated yield

According to the results, various aldehydes were utilized successfully in both types of reactions, and the related products were obtained in high yields.

The stability of the Fe_3O_4@L-proline was examined for sequential recyclability in the condensation of thiophene-2-carbaldehyde, malononitrile, and dimedone to the corresponding product under the optimized reaction conditions.

The results indicated that, the Fe_3O_4@L-proline was recycled up to five cycles without any noticeable loss of its

catalytic performance (Figure 8). In addition, the IR spectrum of the

recovered nano bio-catalyst was as the same as the fresh catalyst.

Figure 8. The recycling of Fe_3O_4@L-proline for the condensation of thiophene-2-carbaldehyde, malononitrile and dimedone in water.

In order to compare the catalytic performance of the Fe_3O_4@L-proline in the synthesis of tetrahydrobenzo[*b*]pyrans with some

other reported catalysts, the reaction conditions and products' yields were tabulated (Table 4).

Table 4. Comparison of the condensation of three component aldehydes, malononitrile and dimedone catalyzed by Fe_3O_4@L-proline with those obtained by the some other reported catalysts

Entry	Catalyst	Reaction Conditions	Time (min)	Yield (%)	Ref.
1	(S)-Proline	H_2O/EtOH	30	78-98	[19]
2	NaBr	Solvent free; MW; 70-80°C	10-15	85-95	[8]
3	Hexadecyldimethylbenzyl ammonium bromide (HDMBAB)	H_2O	420-480	84-93	[20]
4	Na_2SeO_4	EtOH/H_2O; reflux	45-180	80-98	[21]
5	Tetra-methyl ammonium hydroxide (TMAH)	H_2O; r.t.	30-120	80-92	[22]
6	MgO	EtOH/H_2O	22-33	90-96	[23]
7	SiO_2-Pr-SO_3H	H_2O	8-20	88-97	[24]
8	Trisodium citrate	EtOH/H_2O; reflux	5-120	80-96	[25]
9	Silica gel-supported polyphosphoric acid (PPA-SiO_2)	H_2O; reflux	8-15	77-93	[25]
10	Caro's acid-SiO_2	EtOH–H_2O; reflux	15-20	92-95	[26]
11	ZnO-beta zeolite	EtOH; reflux	35-52	86-95	[27]
12	Tetra-n-butylammonium bromide (TBAB)	EtOH; reflux	20-140	87-95	[28]
13	NaOCl	Grinding	10-30	80-88	[29]
14	$Ce_1Mg_xZr_{1-x}O_2$	EtOH; reflux	35-45	90-94	[30]
15	Pentafluoropropionic acid (PFPA)	EtOH/H_2O; r.t.	60-80	89-92	[29]
16	Nano SnO_2	EtOH; r.t.	3-12	92-98	[18]
17	(2-aminomethyl) phenol supported on hydroxyapatite-encapsulated-γ-Fe_2O_3 ([γ-Fe_2O_3@Hap-Si-$(CH_2)_3$-AMP])	H_2O; reflux	10	70-84	[17]
18	1-carboxymethyl-3-methylimidazolium bromide ([cmmim]Br)	Solvent free; 110 °C	1-30	84-97	[31]

19	[pyridine–SO$_3$H]Cl	Solvent free; 95 °C	5-20	86-95	[32]
20	Hexadecyltrimethyl ammonium bromide (HTMAB)	H$_2$O; reflux	180	59-95	[33]
21	NH$_4$OAc	EtOH, r.t.	50	85-93	[34]
22	I$_2$	DMSO, 120 °C	192-240	80-92	[35]
23	2-Hydroxyethylammonium formate	solvent free, r.t.	2-10	43-87	[15]
24	*p*-Dodecylbenzenesulfonic acid (DBSA)	H$_2$O; reflux	240-420	69-90	[14]
25	Fe$_3$O$_4$@L-proline	H$_2$O; reflux	10-15	44-93	This work

As seen in Table 4, the localization of multiple catalytic centers on the nano magnetite cores grant the significant catalytic performance to Fe$_3$O$_4$@L-proline even compared with L-proline as a hemogenouse catalyst (Table 4, Entry 1).

Conclusion

In this research study, we have employed magnetite L-proline as an efficient, reusable and low cost nano-biocatalyst to synthesize 4*H*-benzo[*b*]pyrans in refluxing water. We applied a green protocol for the production of biologically interesting compounds in aqueous media, which could compete with some of the previously reported toxic, expensive, and complicated methods.

Acknowledgments

References

[1] W. Notz, F. Tanaka, C.F. Barbas, *Acc. Chem. Res.*, **2004**, *37*, 580-591.

[2] M. Hirose, S. Sugisaki, K. Suga, H. Umakoshi, *J. Chem.*, **2019**, Article ID 4926435.

[3] M.R. Poor Heravi, P. Aghamohammadi, *CR Chim*., **2012**, *15*, 448-453.

[4] M. Movassaghi, E.N. Jacobsen, *Science*. **2002**, *298*, 1904-1905.

[5] V. Polshettiwar, R. Luque, A. Fihri, H. Zhu, M. Bouhrara, J.-M. Basset, *Chem. Rev.,* **2011**, *111*, 3036-3075.

[6] S. Shylesh, V. Schünemann, W. R. Thiel, *Angew. Chem. Int. Edit.,* **2010**, *49*, 3428-3459.

[7] Y. Chi, Q. Yuan, Y. Li, J. Tu, L. Zhao, N. Li, X. Li, *J. Colloid. Interf. Sci.,* **2012**, *383*, 96-102.

[8] I. Devi, P.J. Bhuyan, *Tetrahedron Lett.,* **2004**, *45*, 8625-8627.

[9] L. Bonsignore, G. Loy, D. Secci, A. Calignano, *Eur. J. Med. Chem.,* **1993**, *28*, 517-520.

[10] C. Konkoy, D. Fick, S. Cai, N. Lan, J. Keana, 2001 PCT international application WO0075123, *Chem Abstr.,* **2000**, *134*, 29313a.

[11] I. Kostova, I. Manolov, I. Nicolova, S. Konstantinov, M. Karaivanova, *Eur. J. Med. Chem.,* **2001**, *36*, 339-347.

[12] Z. H. Chohan, A.U. Shaikh, A. Rauf, C.T. Supuran, *J. Enzyme. Inhib. Med. Chem.,* **2006**, *21*, 741-748.

[13] K. Tabatabaeian, H. Heidari, M. Mamaghani, N.O. Mahmoodi, *Appl. Organomet. Chem.*, **2012**, *26*, 56-61.

[14] E. Sheikhhosseini, D. Ghazanfari, V. Nezamabadi, *Iran. J. Catal.,* **2013**, *3*, 197-201.

[15] H. Shaterian, M. Arman, F. Rigi, *J. Mol. Liq.,* **2011**, *158*, 145-150.

[16] J. Zheng, Y.-Q. Li, *Arch. Appl. Sci. Res.*, **2011**, *3*, 381-388.

[17] M. Khoobi, L. Ma'mani, F. Rezazadeh, Z. Zareie, A. Foroumadi, A.

Ramazani, A. Shafiee, *J. Mol. Catal. A-Chem.,* **2012**, *359*, 74-80.

[18] S.M. Vahdat, M. Khavarpour, F. Mohanazadeh, *J Appl Chem.*, **2015**, *9*, 41-46.

[19] S. Balalaie, M. Bararjanian, A. M. Amani, B. Movassagh, *Synlett.,* **2006**, *2006*, 263-266.

[20] T.-S. Jin, A.-Q. Wang, F. Shi, L.-S. Han, L.-B. Liu, T.-S. Li, *Arkivoc,* **2006**, *14*, 78-86.

[21] R. Hekmatshoar, S. Majedi, K. Bakhtiari, *Catal. Commun.*, **2008**, *9*, 307-310.

[22] S. Balalaie, M. Sheikh-Ahmadi, M. Bararjanian, *Catal. Commun.*, **2007**, *8*, 1724-1728.

[23] M. Seifi, H. Sheibani, *Catal. Lett.,* **2008**, *126*, 275-279.

[24] G.M. Ziarani, A. Abbasi, A. Badiei, Z. Aslani, *J. Chem.,* **2011**, *8*, 293-299.

[25] A. Davoodnia, S. Allameh, S. Fazli, N. Tavakoli-Hoseini, *Chem. Pap.,* **2011**, *65*, 714-720.

[26] H.A. Oskooie, M.M. Heravi, N. Karimi, M.E. Zadeh, *Synth. Commun.,* **2011**, *41*, 436-440.

[27] S.S. Katkar, M.K. Lande, B.R. Arbad, S. T. Gaikwad, *Chin. J. Chem.,* **2011**, *29*, 199-202.

[28] S. Gurumurthi, V. Sundari, R. Valliappan, *J. Chem.,* **2009**, *6*, S466-S472.

[29] N. Montazeri, T. Noghani, M. Ghorchibeigy, R. Zoghi, *J. Chem.,* **2014**, Article ID 596171.

[30] S. Rathod, B. Arbad, M. Lande, *Chin. J. Catal.,* **2010**, *31*, 631-636.

[31] A.R. Moosavi-Zare, M.A. Zolfigol, O. Khaledian, V. Khakyzadeh, M.D. Farahani, H.G. Kruger, *New. J. Chem.,* **2014**, *38*, 2342-2347.

[32] M.A. Zolfigol, A. Khazaei, A.R. Moosavi-Zare, J. Afsar, V. Khakyzadeh, O. Khaledian, *J. Chin. Chem. Soc.,* **2015**, *62*, 398-403.

[33] T.-S. Jin, A.-Q. Wang, X. Wang, J.-S. Zhang, T.-S. Li, *Synlett.,* **2004**, 0871-0873.

[34] K.A. Undale, Y. Park, K. Park, D.H. Dagade, D.M. Pore, *Synlett.,* **2011**, 791-796.

[35] R.S. Bhosale, C.V. Magar, K.S. Solanke, S.B. Mane, S.S. Choudhary, R.P. Pawar, *Synth. Commun.,* **2007**, *37*, 4353-4357.

[36] J. Safaei-Ghomi, S. Zahedi, *Appl. Organomet. Chem.,* **2015**, *29*, 566-571.

[37] L. Zhang, R. He, H.-C. Gu, *Appl. Surf. Sci.*, **2006**, *253*, 2611-2617.

[38] Z. An, W. Zhang, H. Shi, J. He, *J. Catal.,* **2006**, *241*, 319-327.

[39] M. Hong, C. Cai, *J. Chem. Res.,* **2010**, *34*, 568-570.

[40] L. Fotouhi, M.M. Heravi, A. Fatehi, K. Bakhtiari, *Tetrahedron Lett.,* **2007**, *48*, 5379-5381.

[41] D. Kumar, V.B. Reddy, S. Sharad, U. Dube, S. Kapur, *Eur. J. Med. Chem.,* **2009**, *44*, 3805-3809.